



Synthesis and application of a bifunctional hybrid organic–inorganic adsorbent based on polyvinylimidazole-SiO₂/APTMS for the extraction of arsenate in aqueous medium

César Ricardo Teixeira Tarley^{a,b,*}, Guilherme Luiz Scheel^a, Fabio Antônio Cajamarca Suquila^a, Maiyara Carolyne Prete^a, Douglas Cardoso Dragunski^c, Mariana Gava Segatelli^a, Affonso Gonçalves Junior^d, Felipe Augusto Gorla^e

^aDepartamento de Química, Universidade Estadual de Londrina, Rod. Celso Garcia Cid, PR 445 Km 380, Campus Universitário, Londrina, PR, CEP 86051-990, Brazil, Tel. +55 43 3371 4366; Fax: +55 43 3371 4286; emails: tarley@uel.br (C.R.T. Tarley), guilhermescheel@hotmail.com (G.L. Scheel), fabio-cajamarca@hotmail.com (F.A.C. Suquila), mayprete@gmail.com (M.C. Prete), mariana@uel.br (M.G. Segatelli)

^bInstituto Nacional de Ciência e Tecnologia (INCT) de Bioanalítica, Universidade Estadual de Campinas (UNICAMP), Instituto de Química, Departamento de Química Analítica, Cidade Universitária Zeferino Vaz s/n, Campinas, SP, CEP 13083-970, Brazil

^cCentro de Engenharias e Ciências Exatas, Universidade Estadual do Oeste do Paraná, Unioeste, Toledo, PR, CEP 85903-000, Brazil, email: dcdragunski@gmail.com

^dCentro de Ciências Agrárias, Universidade Estadual do Oeste do Paraná, Unioeste, Rua Pernambuco, 1777, Marechal Cândido Rondon, PR, CEP 85960-000, Brazil, email: affonso133@hotmail.com

^eInstituto Federal do Paraná (IFPR), Campus Assis Chateaubriand, Avenida Cívica, 475 Centro Cívico, Assis Chateaubriand, PR, CEP 85935-000, Brazil, email: felipe.gorla@ifpr.edu.br

Received 8 July 2016; Accepted 9 December 2016

ABSTRACT

In the present study, the synthesis and characterization of bifunctional organic–inorganic hybrid adsorbent for As(V) extraction in aqueous medium is described. The hybrid adsorbent was synthesized by coupling free radical addition with sol–gel processing, using 1-vinylimidazole (1-VI) as monomer, (3-aminopropyl)trimethoxysilane (APTMS) as amino functional group, vinyltrimethoxysilane as coupling agent, tetraethoxysilane as inorganic precursor and 2,2'-azoisobutyronitrile as radical initiator. Characterization was performed by Fourier transform infrared spectroscopy, thermogravimetric analysis, scanning electron microscopy and textural analysis (surface area, average pore diameter and pore volume). High As(V) adsorption by hybrid adsorbent was observed in a wide pH range 2–7, which indicates robustness to this parameter. From adsorption kinetic, the As(V) adsorption equilibrium was reached quickly (3 min), indicating a fast mass transfer. The pseudo-second order, Elovich and intraparticle diffusion models showed good adjustments on experimental kinetic data. The maximum adsorption capacity was found to be 15.00 mg g⁻¹, which has been higher than others observed from natural, mineral and synthetic adsorbents. The Langmuir–Freundlich dual model showed the best fit on experimental isotherm data, indicating the presence of energetically heterogeneous binding sites in the materials, most likely ascribed to the amino and imidazole groups from APTMS and 1-VI, respectively. Upon achieving outstanding adsorption of As(V), it appears that hybrid material may present good performance as an adsorbent for packing mini-column in separation and preconcentration analytical methods.

Keywords: Adsorption; As(V); Hydride generation atomic absorption spectrometry (HGAAS); Hybrid adsorbent; Sol–gel process.

* Corresponding author.

1. Introduction

Organic–inorganic hybrid (OIH) materials have been increasingly utilized as new materials with multifunctional features in different field of sciences such as energy, biomedicine, catalysis, optoelectronics, sensor devices, automotive, coating technologies and environmental remediation [1]. The OIH materials have not only the properties themselves of organic polymer and inorganic material, but also the unique properties resulting from mixing them at a nanometer level [2]. These materials are advantageous due to the easy control of the final material properties, including the chemical nature of organic and inorganic phases, the size and morphology of these domains and the nature of interphase interactions [3]. It must be emphasized the difficulty on classifying and defining hybrid materials, principally because their performance relies upon nature of interaction between organic and inorganic components [4]. However, the most common classification of OIH material can be divided into two classes. When the organic and inorganic polymeric portions are embedded through weak forces such as electrostatic interactions, Van der Waals or π – π interactions, the OIH material is classified in class I. In class II, the organic and inorganic components are bonded through covalent bonds [4].

Bearing in mind the hybrid materials applications for adsorption of toxic metals, the last OIH class may present better structural rigidity, mechanical properties and, mainly, higher selective and metal ion adsorption capacity by insertion of binding functional groups through covalent bonds in the materials [5,6]. The sol–gel process using organically modified silane precursors and the self-assembly obtaining mesoporous silicas such as MCM (Mobil Crystalline Materials) and SBA (Santa Barbara Amorphous) have been widely employed to prepare OIH materials focusing on metal ions adsorption [7–10]. Unfortunately, these materials cannot contain properly the properties of both organic and inorganic phases, resulting in a material with properties closest to the inorganic compound because the organic phase does not polymerize [11]. In addition, a literature review reports that the aforementioned hybrid materials prepared by sol–gel and self-assembly process have been functionalized with only one type of functional group [4].

Therefore, the present study purpose was to synthesize and characterize a bifunctional hybrid organic–inorganic adsorbent through the synthesis of polyvinylimidazole–SiO₂/(3-aminopropyl)trimethoxysilane (APTMS) by coupling free radical addition with sol–gel process. 1-Vinylimidazole (1-VI) was used as monomer, APTMS as comonomer, vinyltrimethoxysilane (VTMS) as coupling agent, tetraethoxysilane (TEOS) as inorganic precursor and 2,2'-azoisobutyronitrile (AIBN) as radical initiator. Such synthesis strategy, i.e., the polymerization of organic and inorganic components through covalent bond has been already reported in literature to obtain hybrid adsorbents [11–16]; however, the use of bifunctional binding groups, at the best of our knowledge, has not been reported yet. The feasibility of OIH material was evaluated and explored as adsorbent for arsenate [As(V)] in aqueous medium, which justify the use of 1-VI and APTMS as bifunctional binding groups capable to strongly interact with arsenate [17,18]. The choice of arsenic as element in the present study relies upon its high toxicity in aquatic medium.

Two forms in environmental waters are predominant, [As(III) and As(V)]. Their inorganic forms are more toxic than the organic ones, indicating the importance to remove and determine inorganic arsenic from aqueous medium [19]. Although trivalent specie is more harmful than pentavalent, this latter predominates in aquatic medium and is stable in oxygen rich aerobic environments [20,21]. The synthesized adsorbent was characterized by scanning electron microscopy (SEM), Fourier transform infrared (FTIR), thermogravimetric analysis (TGA) and textural data. The adsorption features of material were assessed by isotherm and kinetic studies.

2. Experimental procedure

2.1. Apparatus

The measurements were performed utilizing a constant flow hydride generator Shimadzu® HVG-1 (Tokyo, Japan) coupled with a flame atomic absorption spectrometer Shimadzu® AA-6601 (Tokyo, Japan) equipped with an arsenic hollow-cathode lamp as radiation source (wavelength: 193.7 nm; current: 14 mA), a deuterium lamp for background correction and using argon as carrier (Hydride generation atomic absorption spectrometry (HGAAS)). To introduce the sample into the equipment, a flow injection system was constructed by an Ismatec® IPC-08 peristaltic pump (Glattbrugg, Switzerland), Tygon® tubes (Courbevoie, France), polyethylene tubes (to propel sample solutions; diameter: 0.8 mm) and a homemade poly(methyl methacrylate) injector-commutator. The pH of samples was measured by a Metrohm® 827 pH lab digital pH meter (Herisau, Switzerland).

An infrared spectrometer Shimadzu® 8300 with Fourier transform (Tokyo, Japan) operating in the transmission mode in the range of 4,000–400 cm⁻¹ (through a conventional KBr pellet technique) and 4 cm⁻¹ of resolution was utilized in order to elucidate the functional groups present in the material. To evaluate the material surface morphology, an SEM was performed in a JEOL® JSM 300-LV (Tokyo, Japan). Before analysis, the polymer had been previously coated with a gold thin layer using Leica® Bal-Tec Med 020 (Wetzlar, Germany) equipment. The material thermal stability was analyzed by TGA using a PerkinElmer® TGA 4000 Thermogravimetric Analyzer (Waltham, USA) in the temperature range of 30°C–800°C at a heating rate of 10°C min⁻¹, under nitrogen atmosphere (20 mL min⁻¹). A surface area and pore size analyzer Quantachrome® Nova Model 1200E (Boynton Beach, USA) automatic nitrogen gas adsorption instrument was utilized to determine the specific surface area, average pore diameter and pore volume. After the sample preheating at 120°C for 4 h, the specific surface area was estimated from nitrogen adsorption isotherms according to the Brunauer–Emmett–Teller (BET) multipoint method, and the average pore diameter as well as the pore volume was determined through the Barrett–Joyner–Halenda (BJH) method.

2.2. Reagents and solutions

The polymer synthesis was accomplished by using TEOS (≥98%), APTMS (97%), VTMS (≥98%), 1-VI (≥99%), methanol (≥99.9%), acetic acid (≥99.8%), hydrochloric acid (≥32%) and AIBN (98%), all acquired from Sigma-Aldrich® (St. Louis,

USA) without previous purification. To prevent any possible contamination, all glassware was kept in a 10% (v/v) HNO₃ solution for 24 h with posterior cleaning with ultrapure water. The 1,000 mg L⁻¹ stock solution of As(V) was prepared from Na₂HAsO₄·7H₂O salt dissolved in ultrapure water, and the working solutions were prepared from appropriated dilutions. Sodium borohydride 2% (m/v) solution was prepared by dissolution of NaBH₄ (Sigma-Aldrich®, ≥99%) in a NaOH 0.5% (m/v) solution. The pH of these solutions was adjusted by dropwise addition of sodium hydroxide, hydrochloric acid and/or nitric acid acquired from Merck® (Darmstadt, Germany).

2.3. Synthesis of organic–inorganic hybrid adsorbent

For the synthesis of OIH adsorbent, 12.96 mmol APTMS and 25.92 mmol 1-VI were mixed in 22.0 mL methanol:acetic acid (9:2, v/v). Afterward, the mixture was kept over magnetically stirring during 1 h before the addition of 38.88 mmol VTMS and 1.83 mmol AIBN. The dissolved oxygen was removed by nitrogen purging for 5 min, and the flask was sealed and kept at 60°C on oil bath for 30 min. Thereafter, 24.00 mmol TEOS previously dissolved in 10.0 mL of methanol and 5.0 mL of 1 mol L⁻¹ HCl was added to the mixture. The polymerization occurred at 60°C during 24 h. The obtained material was removed from the flask, dried at 50°C for 24 h, ground in a mortar and sieved in order to obtain particle sizes between 63 and 150 μm. The schematic representation of synthesis of hybrid polymer and possible interaction with arsenate is depicted in Fig. 1.

2.4. Point of zero charge determination

The point of zero charge (pH_{pzc}) determination was evaluated from batch assays. Aliquots of 25.0 mL of 0.1 mol L⁻¹ KCl solution were stirred with 20.0 mg of hybrid adsorbent during 20 min at different pH values ranging from 2.0 up to 8.0, adjusted with HNO₃ and/or NaOH. The solutions pH values were measured before and after the agitation procedure. A plot pH_{final} vs. pH_{initial} was built, and the pH_{pzc} was determined.

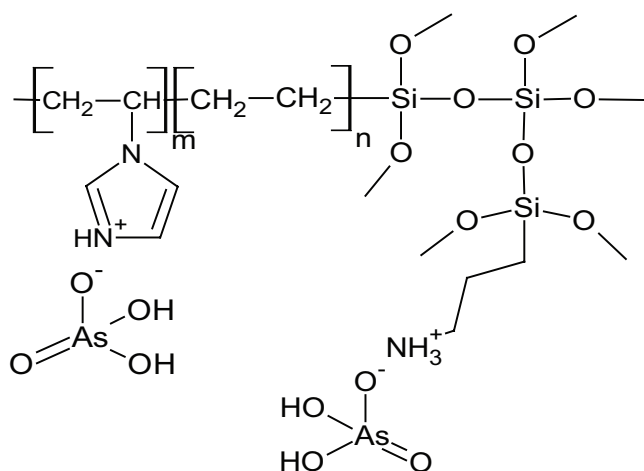


Fig. 1. Schematic representation of hybrid polymer and interaction with As(V).

2.5. Adsorption pH optimization

The pH effect on the adsorptive profile was evaluated from batch assays. Aliquots containing 25.0 mL of 1.0 mg L⁻¹ As(V) solution were stirred for 30 min with 80 mg of material in the following pH values: 2.0, 4.0, 5.0, 5.5, 6.0 and 7.0. Afterward, the mixture was centrifuged at 1,600 rpm for 10 min, and the supernatant was analyzed by HGAAS.

2.6. Adsorption kinetic

The adsorption kinetic studies of As(V) were carried out from batch experiments at room temperature by stirring 100.0 mg of hybrid adsorbent with 25.0 mL of 0.1 mg L⁻¹ As(V) solution at pH 4.00 in different time periods (0.05 until 15 min). After stirring time, the obtained suspensions were centrifuged at 2,000 rpm for 10 min, and the supernatants were used to determine the As(V) retained onto the adsorbent (Q_t , mg g⁻¹), according to Eq. (1):

$$Q_t = \frac{(C_i - C_f)V}{m} \quad (1)$$

where C_i and C_f are the initial and the final (supernatant) As(V) concentrations (mg L⁻¹), respectively, V is the solution volume (L) and m is the adsorbent mass (g). The experimental data were fitted to pseudo-first order, pseudo-second order, kinetics of adsorption study in the regions with constant adsorption acceleration (KASRA), Elovich and intraparticle diffusion models [22,23].

2.7. Adsorption isotherm

In order to build adsorption isotherms, experiments were performed in batch in similar way to kinetic studies: 100.0 mg of hybrid adsorbent were stirred during 3 min with 25.0 mL of As(V) solutions in concentration range varying from 0.05 to 150.00 mg L⁻¹, at pH 4.00 under room temperature. After stirring time, the mixture was centrifuged at 2,000 rpm for 10 min, and the supernatant was used for the determination of arsenate not retained in the hybrid polymer. Eq. (2) was used to determine the amount of arsenate adsorbed onto hybrid polymer.

$$Q_e = \frac{(C_i - C_e)V}{m} \quad (2)$$

where C_i and C_e are the initial and equilibrium As(V) concentrations (mg L⁻¹), respectively, V is the solution volume (L) and m is the adsorbent mass (g). Langmuir, Freundlich, single-site Langmuir–Freundlich and dual-site Langmuir–Freundlich isotherm models were applied to evaluate the data and characterize the arsenate adsorption [24].

2.8. Interference studies

Potential competitive ions on the preconcentration and determination of As(V) were evaluated using a mini-column packed with 50.0 mg of the hybrid material and coupled to a flow injection-hydride generation system. Many co-existing ions were added individually to solutions at pH 4.0 (acetate buffer) containing 0.020 mL⁻¹ As(V) at proportional

concentrations according to the maximum limits recommended by CONAMA 357 (freshwaters, class I) [25]. For this task, the mini-column was loaded with 10.0 mL of each binary solution at a flow rate of 5.0 mL min⁻¹ for 2 min, then eluted with 3.0 mol L⁻¹ HCl, and the desorbed As(V) was online determined by HGAAS. HCl as eluent may be used at concentrations ranging from 1.0 to 3.0 mol L⁻¹, since at very low pH, the As(V) specie is in its molecular form, which has less interaction with the hybrid polymer matrix. However, HCl at 3.0 mol L⁻¹ was chosen for the column elution in order to provide a better peak definition.

3. Results and discussions

3.1. Characterization of organic–inorganic hybrid adsorbent

From the FTIR spectra recorded, some characteristic functional groups of the hybrid adsorbent are observed (Fig. 2). The broad absorption around 3,450 cm⁻¹ can be attributed to $\nu(\text{OH})$ from physically adsorbed water and silanol groups or $\nu(\text{NH})$ from APTMS [26], while the low intensity bands at 3,115 and 2,960 cm⁻¹ refer to $\nu(\text{C-H})$ from APTMS. The band at 1,635 cm⁻¹ corresponds to the $\delta(\text{OH})$ vibration which can be overlapped with C=C stretching from vinyl groups [27]. The presence of bands at 1,504 and 1,413 cm⁻¹ are due to $\nu(\text{C-N})$ and $\nu(\text{C-C})$, respectively, from imidazole ring [11]. The strong band at 1,055 and 439 cm⁻¹ are attributed to $\nu(\text{Si-O})$ from Si-O-Si, indicating the occurrence of hydrolysis and condensation reactions [11,28]. The bands at 921, 763 and 671 cm⁻¹ are assigned to C-H (ring) bending out-of-plane [29].

The adsorbent thermal stability was evaluated by TGA. Thermogravimetric (TG) curves and derivative thermogravimetric (DTG) curves, which are shown in Fig. 3, reveals three well-defined decomposition stages. The first decomposition stage occurs between 30°C and 156°C with a weight loss of 12.8%, attributed to physically adsorbed water on material surface. The second stage was observed between 156°C and 420°C with a weight loss of 17.0%, and can be attributed to the decomposition of poly(1-vinylimidazole) segments [30]. The last stage occurs between 420°C and 700°C due to scission of Si-C present in VTMS and APTMS segments with a weight loss of 16.0%. A ceramic residue of about 53% remains at 800°C, indicating the presence of SiO₂ generated during

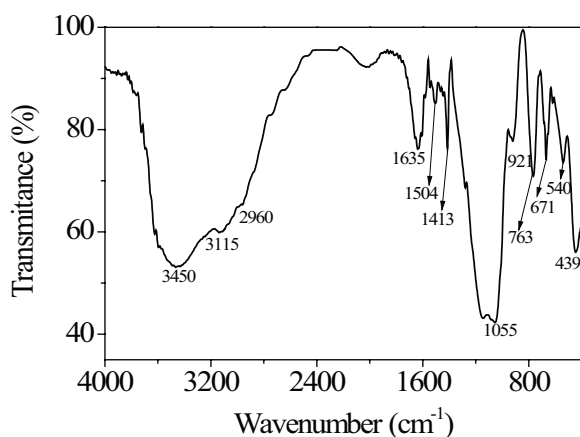


Fig. 2. FTIR spectra for the hybrid sorbent.

heating. This finding indicates larger amount of inorganic material than the achieved to the organic portion.

The surface morphology was evaluated by SEM. As seen in Fig. 4, the ground process gives rise to particles

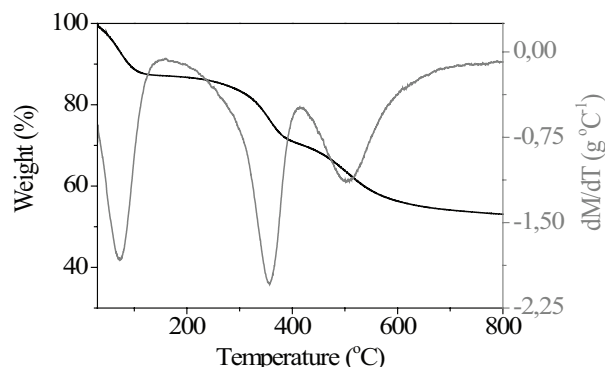


Fig. 3. TG and DTG curves for the hybrid sorbent.

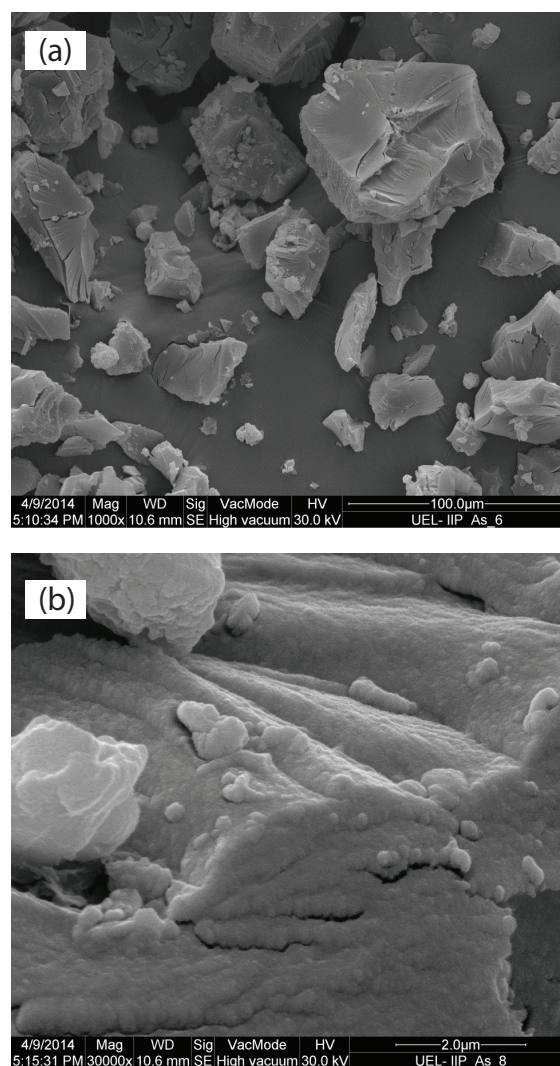


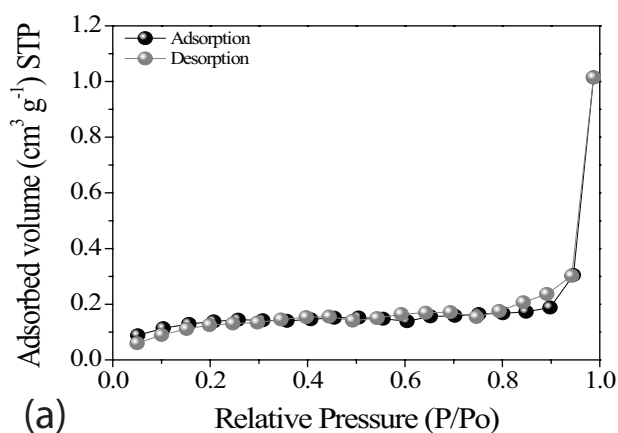
Fig. 4. SEM images for the hybrid sorbent: (a) 1,000 × magnification and (b) 30,000 × magnification.

with irregular shape. Moreover, it is observed the similarity between the adsorbent plane surface with low roughness and an inorganic matrix formed by oxides [31,32], demonstrating once again the larger amount of inorganic portion in the hybrid material.

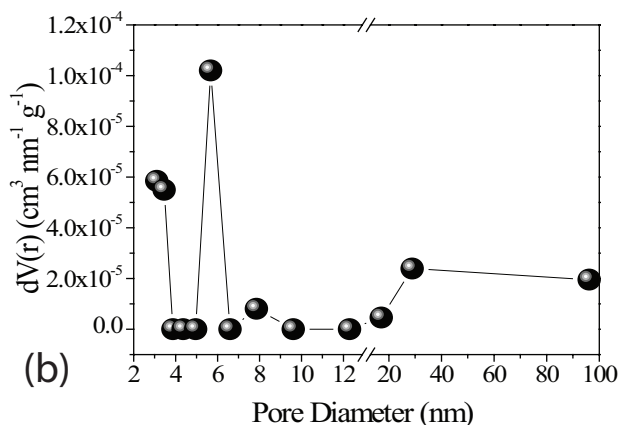
The adsorption isotherm showed no hysteresis, Fig. 5(a), indicating equivalence between condensation and evaporation processes of N_2 gas in the pores material. The hysteresis absence does not indicate no porosity, since some pore formats (such as cylindrical closed in one extremity, conical or channel in “v”) can lead to equals adsorption processes [33]. From BET and BJH data, the surface area, pore volume and pore diameter were obtained and found to be $0.447 \text{ m}^2 \text{ g}^{-1}$, $1.431 \times 10^{-3} \text{ cm}^3 \text{ g}^{-1}$ and 5.672 nm , respectively. According to the pore distribution obtained by the BJH method, Fig. 5(b), it is observed the existence of a well-defined population of pores around 5.671 nm , closer to the average pore diameter. Moreover, the synthesized material presented to be mesoporous by having almost all pore diameters are between 2 and 50 nm [33].

3.2. Point of zero charge remarks

pH_{pzc} is defined as the pH where the electrical charge density on the adsorbent surface is null. The pH_{pzc} was determined by stirring the adsorbent with aqueous solution under



(a) Relative Pressure (P/P_0)



(b)

Fig. 5. (a) Nitrogen adsorption–desorption isotherm and (b) BJH pore size distribution.

different pH values ($\text{pH}_{\text{initial}}$) and the same ionic strength. After stirring time (20 min), the pH_{final} (pH measured in the supernatant) is plotted vs. $\text{pH}_{\text{initial}}$, as shown in Fig. 6. As observed, the pH_{final} remains at pH 3.80 when the $\text{pH}_{\text{initial}}$ was changed from 4.0 up to 8.0, revealing the adsorbent pH_{pzc} value as 3.80. This indicates that at pH values below 3.80 the material surface becomes positively charged and at pH values above 3.80 the polymer surface acquires negative charges capable to adsorb positively charged species. The obtained value showed quite similarity to the pH_{pzc} value of amorphous silica ($\text{SiO}_2 \cdot 2\text{H}_2\text{O}$, $\text{pH}_{\text{pzc}} = 3.50$) [34], comprovig the large amount of inorganic portion in the material, noted earlier by TGA. The slightly increase is justified by the presence of a lower amount of organic portion in the material.

3.3. Influence of pH on the adsorption of As(V) onto organic–inorganic hybrid adsorbent

In order to determine the best conditions for As(V) adsorption onto hybrid adsorbent, a pH study was performed in a range of 2.00–7.00, as shown in Fig. 7. High As(V)

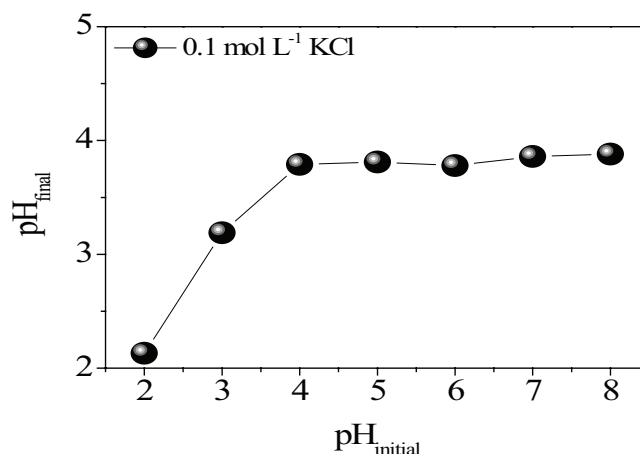


Fig. 6. Point of zero charge (pH_{pzc}) determination of hybrid polymer.

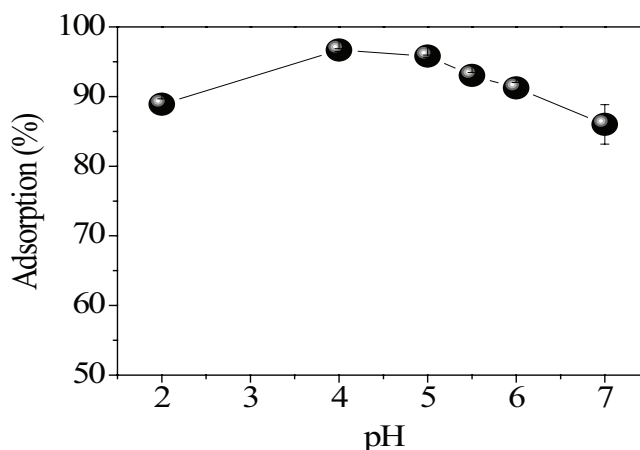


Fig. 7. Effect of pH on the sorption capacity of the hybrid sorbent for As(V) ($n = 2$).

adsorption percentages (around 72%–97%) were obtained for all pH ranges studied, however, it was observed a slightly higher adsorption at pH 4.00. According to the literature, below pH 4.00 the H_3AsO_4 and $H_2AsO_4^-$ species are found, whereas at the pH range of 4.00–6.00 the dominant specie is $H_2AsO_4^-$ and above pH 7.00 is found primarily as $H_2AsO_4^-$ and $HAsO_4^{2-}$ [35].

Since the adsorption process of As(V) onto the adsorbent may takes place through electrostatic interactions between the analyte and material surface [36], the monovalent specie $H_2AsO_4^-$ is more efficiently adsorbed, which can explain the higher adsorption at pH 4.00. At this pH, the As(V) specie presents electrostatic interaction with positively charged amino group, originating from APTMS (pKa = 10.6) and positively charged nitrogen atom from imidazole ring (pKa = 6.26) [22]. On the other hand, at pH 7.00 the imidazole ring suffers deprotonation, and, as consequence, gives rise to repulsion forces with $H_2AsO_4^-$ and $HAsO_4^{2-}$, which may explain the lower adsorption of As(V) in the adsorbent. However, the rather low difference on the adsorption percentage (10.6%) between pH 4.00 and 7.00 clearly shows the important role of amino group from APTMS on the As(V) adsorption, since the amino group exists in its completely protonated form while the imidazole is found only 24% in its protonated form at pH 7.00. This finding can be ascribed to the higher amount of inorganic portion in the hybrid material, as has already been mentioned. At pH 2.00, As(V) exists in its molecular form (H_3AsO_4) and $H_2AsO_4^-$ by being near its first acid dissociation constant (pKa = 2.2) while the material surface (vinylimidazole, binding sites from APTMS and inorganic portion) acquires predominantly positive charge. The As(V) retention under this medium is also explained by electrostatic interaction, however, with lower adsorption due to the presence of molecular form.

3.4. Adsorption kinetics

An adsorption kinetic study has significant importance because it provides information about the adsorption process mechanisms. The adsorption equilibrium effect between the solid and liquid phases was reached in 3 min, Fig. 8, indicating

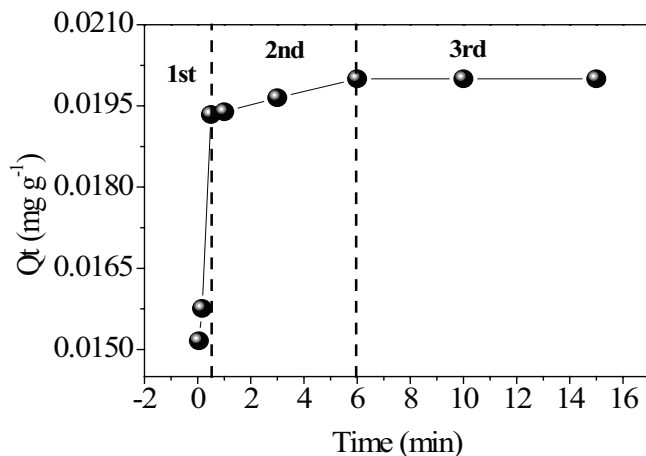


Fig. 8. Kinetic curve of arsenate sorption onto the hybrid sorbent under stirring.

a fast mass transfer of As(V) from the solution toward the adsorptive site. In order to investigate the kinetic mechanism driving As(V) toward the surface of hybrid material a pseudo-first order, pseudo-second order, KASRA, Elovich and intraparticle diffusion kinetic models were applied.

The pseudo-first-order model is given by Eq. (3) as follows:

$$\log(Q_e - Q_t) = \log Q_e - \frac{k_1}{2.303} t \quad (3)$$

where k_1 is the pseudo-first-order sorption rate constant (min^{-1}), Q_e and Q_t are the concentration of adsorbate at equilibrium and a determined time, respectively and t is the adsorption time (min). This model has been widely utilized to describe adsorption behavior when the occupation rate of adsorption sites is proportional to the number of unoccupied sites and assumes the adsorption occurrence at energetically homogeneous sites on the adsorbent surface [37]. Due to the equality between the occupation of adsorption sites and the number of unoccupied ones, this model infers a good adjustment to the initial adsorption because the amounts of free binding sites are much higher when compared with equilibrium conditions [38].

The pseudo-second-order equation is given by Eq. (4) as follows:

$$\frac{t}{Q_t} = \frac{1}{k_2 Q_e^2} + \frac{1}{Q_e} t \quad (4)$$

where k_2 is the pseudo-second-order sorption rate constant ($\text{g mg}^{-1} \text{min}^{-1}$), Q_e and Q_t are the concentration of adsorbate at equilibrium and determined time, respectively and t is the adsorption time (min). Different from the pseudo-first-order model, the pseudo-second order infers the possibility of predicting the adsorption through all its extent when the adsorption capacity is proportional to the number of active binding sites occupied with different energy [39].

In order to explore the adsorption kinetic data, the KASRA model “kinetics of adsorption study in the regions with constant adsorption acceleration” was applied [40]. This model considers: (1) each time range, which the adsorption acceleration in constant, is named as “region”; (2) the existence of two regions before attaining plateau region and (3) the boundaries between the first and second regions and the second and third (plateau) regions are determined by the KASRA equation:

$$Q_t = At^2 + Bt + C \quad (5)$$

where $A = 1/2 a_i$, $B = v_{0i} - a_i t_{0i}$, $C = Q_{0i} - 1/2 a_i t_{0i}^2 - (v_{0i} - a_i t_{0i}) t_{0i}$, a_i is acceleration of adsorption kinetic in the i -th region and $i = 1-3$, v_{0i} and t_{0i} are the velocity and time values in the beginning of i -th region, respectively, Q_{0i} is the Q_t value in the beginning of i -th region.

The Elovich equation is given by Eq. (6) as follows:

$$Q_t = \frac{1}{\beta} \ln(\alpha\beta) + \frac{1}{\beta} \ln t \quad (6)$$

where t is the adsorption time (min), Q_t is the concentration of adsorbate at determined time, β is the extent of surface coverage and activation energy for adsorption (g mg^{-1}) and α is the initial adsorption rate constant ($\text{min}^{-1} \text{mg g}^{-1}$). The Elovich has also been used to describe the adsorption of inorganic compounds from aqueous medium and it assumes an adsorbent surface energetically heterogeneous due to the presence of different binding sites through chemisorption [41].

In order to evaluate if the As(V) adsorption process onto hybrid polymer is controlled by intraparticle diffusion, external surface adsorption or both adsorption mechanisms, the intraparticle diffusion model given by Eq. (7) was evaluated to the experimental data:

$$Q_t = k_{id}t^{1/2} + C \quad (7)$$

where C is the boundary layer thickness (mg g^{-1}), Q_t is the adsorbate concentration at determined time and k_{id} is the internal diffusion coefficient ($\text{mg g}^{-1} \text{min}^{-1/2}$). From this model a good fit to the experimental data is observed when C parameter is equal to zero, indicating the adsorption process occurrence only by intraparticle diffusion. When C parameter is far from zero, the existence of multilinear segments indicates external surface adsorption and intraparticle diffusion [42].

The kinetics parameters values obtained from the theoretical models as well as the determination coefficient (R^2) are summarized in Table 1. As expected, the pseudo-second-order model had a good adjustment to experimental data, indicating the occurrence of arsenate adsorption on a heterogeneous surface containing adsorption sites with different binding energies attributed to positively charged amino group and nitrogen atom from imidazole ring. This applied model presented a satisfactory determination coefficient and a predicted maximum adsorption capacity ($Q_e = 0.020 \text{ mg g}^{-1}$) very similar to the experimental data ($Q_e = 0.019 \text{ mg g}^{-1}$). The Elovich model lack of fit reveals an As(V) adsorption not described by chemisorption, but most likely through electrostatic interaction.

As observed from Fig. 8 and Table 1, two regions before plateau can be observed according to KASRA equation. In the first region, the positive value for a_i indicates that the initial adsorption of adsorbate molecules facilitates adsorption of other ones and the interaction between them acts as a driving force. From the first region to the second one, with increase in time, v_{0i} values decreased and a_i values became negative, indicating the decreasing of the number of surface adsorption sites and As(V) concentration [40]. As regard the intraparticle diffusion model, it can be observed two linear segments with good regression coefficients, indicating the existence of two adsorption stages attributed to quick external surface adsorption and the intraparticle diffusion through pores of hybrid material.

3.5. Adsorption isotherms

To estimate the maximum adsorption capacity of hybrid polymer toward the As(V), it was necessary to build adsorption isotherm. In reported literature, the use of non-linear isotherms represents a viable and powerful tool for improving the interpretation of adsorption data, because it avoids some errors on the parameters when linearized models are employed [43].

Table 1
Kinetics parameters values to kinetics models applied in the experimental data

Model	Parameters	Values
Pseudo-first order	Q_e	2.6×10^{-3}
	k_1	7.8×10^{-1}
	R^2	0.6
Pseudo-second order	Q_e	20.0×10^{-3}
	k_2	1.6×10^3
	R^2	1.00
KASRA first region	A	1.3×10^{-2}
	B	2.1×10^{-3}
	C	15.0×10^{-3}
	a_1	6.5×10^{-3}
	v_{01}	2.5×10^{-3}
KASRA second region	A	-1.4×10^{-6}
	B	1.3×10^{-4}
	C	19.3×10^{-3}
	a_2	-6.9×10^{-7}
	v_{02}	1.3×10^{-4}
Elovich	β	7.8×10^2
	α	2.1×10^9
	R^2	0.834
Intraparticle diffusion	k_{id}	8.9×10^{-3}
	C	1.3×10^{-2}
	R^2	0.931
	k_{id}	4.2×10^{-4}
	C	1.9×10^{-2}
	R^2	0.99

Note: Experimental $Q_e = (0.019 \text{ mg g}^{-1})$. k_1 : pseudo-first-order constant of the adsorption process (min^{-1}); k_2 : pseudo-second-order constant of the adsorption process ($\text{g mg}^{-1} \text{min}^{-1}$); a_i : acceleration of adsorption kinetic in the first region; v_{0i} : velocity in the first region; a_i : acceleration of adsorption kinetic in the second region; v_{0i} : velocity in the second region; β : extent of surface coverage and activation energy for adsorption (g mg^{-1}); α : initial adsorption rate constant ($\text{mg g}^{-1} \text{min}^{-1}$); k_{id} : internal diffusion coefficient ($\text{mg g}^{-1} \text{min}^{-1/2}$) and C : constant related with the boundary layer thickness (mg g^{-1}).

The non-linear Langmuir model is described by Eq. (8) and admits the presence of homogeneous binding sites, whereas the adsorption occurs by the formation of a monolayer on the adsorbent surface. In this equation, the Q_e is the adsorptive capacity of each studied concentration (mg g^{-1}), K_L is the Langmuir constant (L mg^{-1}), b is the maximum adsorptive capacity (mg g^{-1}) and C_e is the equilibrium concentration (mg L^{-1}) [20,44].

$$Q_e = \frac{K_L b C_e}{(1 + LC_e)} \quad (8)$$

In the non-linear Freundlich model, Eq. (9), the adsorption process occurs by forming multilayers on the adsorbent surface, consequently not predicting the adsorbent saturation. This model is used to describe heterogeneous process, in which $1/n$ represents the factor heterogeneity and K_f is the Freundlich constant (L mg^{-1}) [21].

$$Q_e = K_F (C_e)^{1/n} \tag{9}$$

In order to confirm the availability of heterogeneous and homogeneous sites capable to adsorb As(V), i.e., the presence of adsorption binding sites with different affinities, the hybrid Langmuir–Freundlich model was applied to the experimental data (Eq. (10)). In this equation, b represents the maximum adsorptive capacity (mg g^{-1}), K is the constant of adsorption affinity (L mg^{-1}), n is the factor heterogeneity, C_e is the equilibrium concentration (mg L^{-1}) and Q_e represents the adsorptive capacity (mg g^{-1}) [20]. Such hybrid model is useful to describe both the Langmuir type and Freundlich type. In order words, at low concentrations of adsorbate, the model reduces to a Freundlich isotherm, while at high concentrations it behaves as a Langmuir isotherm giving rise to a monolayer until the maximum adsorption capacity is achieved.

$$Q_e = \frac{b(K_1 C_e)^{n_1}}{1 + (K_1 C_e)^{n_1}} \tag{10}$$

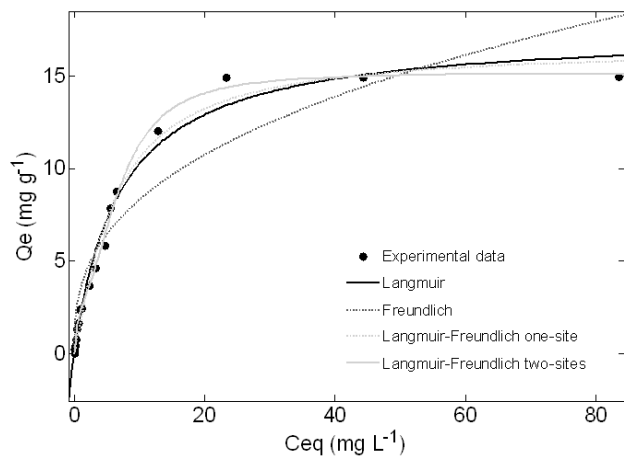


Fig. 9. Isotherms plots for arsenate sorption onto hybrid sorbent under stirred during 3 min, pH 4.00 and room temperature.

The presence of heterogeneous and homogeneous binding sites by using the Langmuir–Freundlich single model can be evaluated through the analysis of index n , which can vary from 0 to 1. It is acceptable the presence of homogeneous binding sites when the index n is close to 1, while when it is less than 1 the material has heterogeneous sites. Although widely used, the Langmuir–Freundlich single model is not able to determine the presence of two-adsorption sites with different affinities toward adsorbate. On the other hand, the Langmuir–Freundlich dual equation, as demonstrated by Eq. (11), makes possible to elucidate the presence of heterogeneous solid surface and the availability of higher-affinity and lower-affinity sites [16,45].

$$Q_e = \frac{b_1(K_1 C_e)^{n_1}}{1 + (K_1 C_e)^{n_1}} + \frac{b_2(K_2 C_e)^{n_2}}{1 + (K_2 C_e)^{n_2}} \tag{11}$$

From the experimental adsorption isotherm depicted in Fig. 9, the maximum adsorption capacity observed for the hybrid adsorbent was found to be 15.0 mg g^{-1} . The adsorption parameters obtained for the theoretical models applied to the experimental data are presented in Table 2. The Langmuir–Freundlich dual model showed best fit to the experimental data due to lowest root mean square error, higher determination coefficient ($R^2 = 0.9972$) and very similar maximum adsorption capacity ($b_1 + b_2 = 15.22 \text{ mg g}^{-1}$) to the experimental Q_e (15.00 mg g^{-1}), allowing to estimate the availability of more than one type of adsorption sites. Those findings corroborates to the kinetic study, where the heterogeneous surface with different binding energies is attributed to positively charged amino group and nitrogen atom from imidazole ring.

Besides, it should be noted that the difference between the parameters K_1 and K_2 (adsorbate – adsorbent affinities) is rather high (0.14 and 2.02 L g^{-1}), confirming the differences on the affinity of amino group and nitrogen atom toward the As(V) adsorption. Higher adsorption of As(V) was achieved at lower-affinity binding site ($K_1 = 0.14 \text{ L g}^{-1}$ and $b_1 = 12.34 \text{ mg g}^{-1}$), while a low amount of adsorption was observed at higher-affinity binding site ($K_2 = 2.02 \text{ L g}^{-1}$ and $b_2 = 2.88 \text{ mg g}^{-1}$). Based on the achieved results, bearing in mind the larger amount of inorganic matrix on the hybrid adsorbent, we can infer that

Table 2
Adsorption parameters values to adsorption models applied to the experimental data

Model	Equation	K_1	K_2	b_1	b_2	n_1	n_2	R^2	RMSE
Non-linear Langmuir	$Q_e = \frac{K_L b C_e}{(1 + L C_e)}$	0.14	–	17.48	–	–	–	0.9857	0.68
Non-linear Freundlich	$Q_e = K_F (C_e)^{1/n}$	3.54	–	–	–	0.37	–	0.9044	1.76
Langmuir–Freundlich single site	$Q_e = \frac{b(K_1 C_e)^{n_1}}{1 + (K_1 C_e)^{n_1}}$	0.16	–	16.55	–	1.18	–	0.9877	0.65
Langmuir–Freundlich dual sites	$Q_e = \frac{b(K_1 C_e)^{n_1}}{1 + (K_1 C_e)^{n_1}} + \frac{b(K_2 C_e)^{n_2}}{1 + (K_2 C_e)^{n_2}}$	0.14	2.02	12.34	2.88	2.20	1.59	0.9972	0.35

Note: Experimental $Q_e = (15.0 \text{ mg g}^{-1})$. In the Langmuir, Freundlich and Langmuir–Freundlich equations: K_L (Langmuir), $K_{1,2}$ (Langmuir–Freundlich) (L g^{-1}), K_F (Freundlich) (mg g^{-1}) (L g^{-1}) are adsorbate – adsorbent affinities, b , $b_{1,2}$ are maximum adsorption capacities (mg g^{-1}) and n , $n_{1,2}$ are intensities or degrees of favorability for adsorption. RMSE is the root mean square error.

the lowest affinity site for the As(V) adsorption is attributed to the APTMS while the highest one is ascribed to nitrogen atom from imidazole ring, even though the former one is found in high amount in the polymeric network. This finding is still assured by Langmuir–Freundlich single model analysis, recognizing the As(V) adsorption occurrence only at the lower-affinity binding site attributed to APTMS as a result of its higher amount. However, the Langmuir–Freundlich single model analysis fails on describing the adsorption at higher-affinity binding site.

Comparing the experimental maximum adsorption capacity with a wide range of materials including natural and synthetic adsorbents reported in literature (Table 3), the unprecedented hybrid adsorbent exhibits satisfactory performance for As(V) adsorption in aqueous medium. It is worth to emphasize the highest adsorption capacity of this proposed hybrid material when compared with inorganic polymer mesoporous silica modified with 3-(2-aminoethylamino) propyltrimethoxysilane previously reported [19], confirming the effectiveness and importance of hybrid adsorbents for removing pollutants.

3.6. Interference studies

In order to evaluate the effect of competitive ions, As(V) determination on binary solutions was compared with a solution containing only As(V) at the same concentration. It was found that in the presence of 20.0 mg L⁻¹ NO₃⁻, 2.0 mg L⁻¹ NO₂⁻, 0.600 mg L⁻¹ Fe³⁺, 0.050 mg L⁻¹ Ni²⁺, 0.200 mg L⁻¹ Al³⁺, 0.020 mg L⁻¹ Pb²⁺ and Se⁴⁺ no significant difference was observed on As(V) determination, considering a relative error of 10%. However, in the presence of 500.0 mg L⁻¹ SO₄²⁻, 500.0 mg L⁻¹ Cl⁻ and 0.360 mg L⁻¹ Zn²⁺, the As(V) determination was negatively affected by 70%, 25% and 50%, respectively, which is mostly likely

Table 3
Comparative data of some materials (natural and synthetic) for the arsenate adsorption in aqueous medium

Adsorbents	Q _e (mg g ⁻¹)	References
Hybrid organic–inorganic adsorbent	15.00	This work
3-(2-Aminoethylamino) propyltrimethoxysilane modified ordered mesoporous silica	10.3	[19]
Nickel/nickel boride nanoparticles coated resin	17.80	[46]
Surface-ion-imprinted amine-functionalized silica gel	16.10	[47]
Pine leaves	3.27	[48]
Chitosan	0.73	[49]
Agricultural residue ‘rice polish’	0.147	[50]
Fe–zeolite	0.11	[51]
Biochar (derived from rice husk)	7.10	[52]
Al-impregnated activated alumina	3.00	[53]

Note: Q_e is the maximum adsorption capacity.

attributed to interferences on hydride generation system, since the same interference was noticed without the pre-concentration step.

4. Conclusions

In this paper it is described the synthesis, characterization and application of a new hybrid polymer based on polyvinylimidazole-SiO₂/APTMS as adsorbent for As(V) in aqueous medium. The characteristic adsorption of the hybrid bifunctional adsorbent was evaluated from batch assays by exploiting kinetic and isotherm studies, where the presence of heterogeneous solid surface on the material containing higher-affinity and lower-affinity sites was confirmed. Although higher inorganic amount in the material has been achieved, giving rise to larger adsorption of As(V) by the amino group from APTMS, this binding site possesses low affinity toward the As(V). The material presented a slightly rough morphology, conferred a fast mass transfer (3 min) and a high maximum adsorption capacity (15.00 mg g⁻¹) when compared with other adsorbents in literature. One should note the satisfactory cost for manufacturing the hybrid polymer. Considering the cost of reagents from Sigma-Aldrich, 1 kg of material can be synthesized by a cost of US\$ 269, which is lower than commercial adsorbent for As(V) adsorption Amberlyst® A21 free base styrene divinylbenzene modified with dimethylamino (1 kg = US\$ 514). For final remarks, the mini-column packed with the hybrid polymer may be used up to 150 times without any change on its performance, indicating the high reusability of hybrid polymer.

Acknowledgments

The authors acknowledge the financial support of Conselho Nacional de Desenvolvimento Científico e Tecnológico (CNPq) (Project No. 481669/2013-2, 305552/2013-9, 472670/2012-3), Coordenação de Aperfeiçoamento de Pessoal de Nível Superior (CAPES), Fundação Araucária do Paraná/SANEPAR (163/2014) and Instituto Nacional de Ciência e Tecnologia de Bioanalítica (INCT) (Project No. 573672/2008-3).

References

- [1] T. Krasia-Christoforou, Organic-Inorganic Polymer Hybrids: Synthetic Strategies and Applications, In: T. Sano, C.L. Randow, C-S. Kim, Hybrid and Hierarchical Composite Materials, Springer, Heidelberg, 2015, pp. 11–63.
- [2] T. Ogoshi, H. Itoh, K. Kim, M.Y. Chujo, Thermal and solvent-resistant properties of organic–inorganic polymer hybrids having interpenetrating polymer network structure by formation of metal–bipyridyl complex, *Polymer*, 35 (2003) 178–184.
- [3] D. Saikia, C.G. Wu, J. Fang, L.D. Tsai, H.M. Kao, Organic–inorganic hybrid polymer electrolytes based on polyether diamine, alkoxysilane, and trichlorotriazine: synthesis, characterization, and electrochemical applications, *J. Power Sources*, 269 (2014) 651–660.
- [4] B. Samiey, C-H. Cheng, J. Wu, Organic-inorganic hybrid polymers as adsorbents for removal of heavy metal ions from solutions: a review, *Materials*, 7 (2014) 673–726.
- [5] P. Gómez-Romero, C. Sanches, *Functional Hybrid Materials*, Wiley-VCH Verlag, Weinheim, 2004.
- [6] L. Mercier, T.J. Pinnavaia, Heavy metal ion adsorbents formed by the grafting of a thiol functionality to mesoporous silica molecular sieves: factors affecting Hg(II) uptake, *Environ. Sci. Technol.*, 32 (1998) 2749–2754.

- [7] H.-T. Fan, W. Sun, B. Jiang, Q.-J. Wang, D.-W. Li, C.-C. Huang, K.-J. Wang, Z.-G. Zhang, W.-X. Li, Adsorption of antimony(III) from aqueous solution by mercapto functionalized silica-supported organic-inorganic hybrid sorbent: mechanism insights, *Chem. Eng. J.*, 286 (2016) 128–138.
- [8] L. Giraldo, J.C. Moreno-Piraján, Study on the adsorption of heavy metal ions from aqueous solution on modified SBA-15, *Mater. Res.*, 16 (2013) 745–754.
- [9] M. Najafi, Y. Yousefi, A.A. Rafati, Synthesis, characterization and adsorption studies of several heavy metal ions on amino-functionalized silica nano hollow sphere and silica gel, *Sep. Purif. Technol.*, 85 (2012) 193–205.
- [10] V. Parvulescu, M. Muresanu, A. Reiss, R. Ene, S.-H. Suh, Metal-organic hybrids obtained by functionalization of mesoporous silica, *Rev. Roum. Chim.*, 55 (2010) 1001–1008.
- [11] C.R.T. Tarley, F.N. Andrade, F.M. de Oliveira, M.Z. Corazza, L.F.M. de Azevedo, M.G. Segatelli, Synthesis and application of imprinted polyvinylimidazole-silica hybrid copolymer for Pb²⁺ determination by flow-injection thermospray flame furnace atomic absorption spectrometry, *Anal. Chim. Acta*, 703 (2011) 145–151.
- [12] K.M. Diniz, M.G. Segatelli, C.R.T. Tarley, Synthesis and adsorption studies of novel hybrid mesoporous copolymer functionalized with protoporphyrin for batch and on-line solid-phase extraction of Cd²⁺ ions, *React. Funct. Polym.*, 73 (2012) 838–846.
- [13] C.R.T. Tarley, F.N. Andrade, H. Santana, D.A.M. Zaia, L.A. Beijo, M.G. Segatelli, Ion-imprinted polyvinylimidazole-silica hybrid copolymer for selective extraction of Pb(II): characterization and metal adsorption kinetic and thermodynamic studies, *React. Funct. Polym.*, 72 (2012) 83–91.
- [14] C.I. Lin, A.K. Joseph, C.K. Chang, U.C. Wang, Y.D. Lee, Synthesis of molecular imprinted organic-inorganic hybrid polymer binding caffeine, *Anal. Chim. Acta*, 481 (2003) 175–180.
- [15] P.J. Skrdla, M. Shnayderman, L. Wright, T.P. O'Brien, GC-MS Study of the formation of alkoxyxilanes from a sol-gel precursor in a hydrophobic solution: a potential new route to hybrid molecular imprinted polymers, *J. Non-Cryst. Solids*, 352 (2006) 3302–3309.
- [16] D.N. Clausen, I.M.R. Pires, C.R.T. Tarley, Improved selective cholesterol adsorption by molecularly imprinted poly(methacrylic acid)/silica (PMAA-SiO₂) hybrid material synthesized with different molar ratios, *Mater. Sci. Eng. C*, 44 (2014) 99–108.
- [17] Y.K. Tsoi, Y.M. Ho, K.S. Leung, Selective recognition of arsenic by tailoring ion-imprinted polymer for ICP-MS quantification, *Talanta*, 89 (2012) 162–168.
- [18] F. Zheng, B. Hu, Dual silica monolithic capillary microextraction (CME) on-line coupled with ICP-MS for sequential determination of inorganic arsenic and selenium species in natural waters, *J. Anal. At. Spectrom.*, 24 (2009) 1051–1061.
- [19] D. Chen, C. Huang, M. Hen, B. Hu, Separation and preconcentration of inorganic arsenic species in natural water samples with 3-(2-aminoethylamino) propyltrimethoxysilane modified ordered mesoporous silica micro-column and their determination by inductively coupled plasma optical emission spectrometry, *J. Hazard. Mater.*, 164 (2009) 1146–1151.
- [20] A.O. Dada, A.P. Olalekan, A.M. Olatunya, O. Dada, Langmuir, Freundlich, Temkin and Dubinin-Radushkevich isotherms studies of equilibrium sorption of Zn²⁺ onto phosphoric acid modified rice husk, *IOSR J. Appl. Chem.*, 3 (2012) 38–45.
- [21] Y.C. Wong, Y.S. Szeto, W.H. Cheung, G. McKay, Adsorption of acid dyes on chitosan—equilibrium isotherm analyses, *Process Biochem.*, 39 (2004) 693–702.
- [22] C.R.T. Tarley, M.Z. Corazza, B.F. Somera, M.G. Segatelli, Preparation of new ion-selective cross-linked poly(vinylimidazole-co-ethylene glycol dimethacrylate) using a double-imprinting process for the preconcentration of Pb²⁺ ions, *J. Colloid Interface Sci.*, 450 (2015) 254–263.
- [23] B. Samiey, A.D. Tehrani, Study of adsorption of janus green b and methylene blue on nanocrystalline cellulose, *J. Chin. Chem. Soc.*, 62 (2015) 149–162.
- [24] E. Galunin, J. Ferreti, I. Zapeline, I. Vieira, C.R.T. Tarley, T. Abrão, M.J.S. Yabe, Cadmium mobility in sediments and soils from a coal mining area on Tibagi River watershed: environmental risk assessment, *J. Hazard. Mater.*, 265 (2014) 280–287.
- [25] CONAMA—Brazilian Environmental Council (2005) Resolution No. 357 (in Portuguese). Available at: <http://www.mma.gov.br/port/conama/res/res05/res35705.pdf> (Accessed on 07.11.2016).
- [26] I.M. El Nahhal, M.M. Chehimi, C. Cordier, G. Dobin, XPS, NMR and FTIR structural characterization of polysiloxane-immobilized amine ligand systems, *J. Non-Cryst. Solids*, 275 (2000) 142–146.
- [27] N.M. El-Ashgar, I.M. El-Nahhal, M.M. Chehimi, F. Babonneau, J. Livage, A new route synthesis of immobilized-polysiloxane iminodiacetic acid ligand system, its characterization and applications, *Mater. Lett.*, 61 (2007) 4553–4558.
- [28] R.J. Fonseca, M.G. Segatelli, K.B. Borges, C.R.T. Tarley, Synthesis and evaluation of different adsorbents based on poly(methacrylic acid-trimethylolpropane trimethacrylate) and poly(vinylimidazole-trimethylolpropane trimethacrylate) for the adsorption of tebuthiuron from aqueous medium, *React. Funct. Polym.*, 93 (2015) 1–9.
- [29] E.F. dos Reis, F.S. Campos, A.P. Lage, R.C. Leite, L.G. Heneine, W.L. Vasconcelos, Z.I.P. Lobato, H.S. Mansur, Synthesis and characterization of poly (vinyl alcohol) hydrogels and hybrids for rMPB70 protein adsorption, *Mater. Res.*, 9 (2006) 185–191.
- [30] T.C. Chang, Y.T. Wang, Y.S. Hong, H.B. Chen, J.C. Yang, Organic-inorganic hybrid materials 7: characterization and degradation of polyvinylimidazole-silica hybrids, *Polym. Degrad. Stab.*, 69 (2000) 317–322.
- [31] G.F. Lima, M.O. Ohara, D.C. Nóbile, D.R. Nascimento, M.G. Segatelli, M.A. Bezerra, C.R.T. Tarley, Flow injection on-line minicolumn preconcentration and determination of trace copper ions using an alumina/titanium oxide grafted silica matrix and FAAS, *Microchim. Acta*, 178 (2012) 61–70.
- [32] C.R.T. Tarley, G.F. Lima, D.R. Nascimento, A.R.S. Assis, E.S. Ribeiro, K.M. Diniz, M.A. Bezerra, M.G. Segatelli, Novel on-line sequential preconcentration system of Cr(III) and Cr(VI) hyphenated with flame atomic absorption spectrometry exploiting sorbents based on chemically modified silica, *Talanta*, 100 (2012) 71–79.
- [33] K.S.W. Sing, D.H. Everett, R.A.W. Haul, L. Moscou, R.A. Pierotti, J. Rouquerol, T. Siemieniowska, Reporting physisorption data for gas/solid systems with special reference to the determination of surface area and porosity, *Pure Appl. Chem.*, 57 (1985) 603–619.
- [34] M.E. Essington, *Soil and Water Chemistry: An Integrative Approach*, CRC Press, Boca Raton, 2004.
- [35] E.O. Kartinen, C.J. Martin, An overview of arsenic removal processes, *Desalination*, 103 (1995) 79–88.
- [36] X. Yu, S. Tong, M. Ge, L. Wu, J. Zuo, C. Cao, W. Song, Synthesis and characterization of multi-amino-functionalized cellulose for arsenic adsorption, *Carbohydr. Polym.*, 92 (2013) 380–387.
- [37] F.M. de Oliveira, M.G. Segatelli, C.R.T. Tarley, Hybrid molecularly imprinted poly(methacrylic acid-TRIM)-silica chemically modified with (3-glycidyoxypropyl)trimethoxysilane for the extraction of folic acid in aqueous medium, *Mater. Sci. Eng. C*, 59 (2015) 643–651.
- [38] Z. Aksu, S. Tezer, Equilibrium and kinetic modelling of biosorption of Remazol Black B by *Rhizopus arrhizus* in a batch system: effect of temperature, *Process Biochem.*, 36 (2006) 431–439.
- [39] W. Plazinski, W. Rudzinski, A. Plazinska, Theoretical models of sorption kinetics including a surface reaction mechanism: a review, *Adv. Colloid Interface Sci.*, 152 (2009) 2–13.
- [40] L. Yan, K. Yang, R. Shan, T. Yan, J. Wei, S. Yu, B. Du, Kinetic, isotherm and thermodynamic investigations of phosphate adsorption onto core-shell Fe₃O₄@LDHs composites with easy magnetic separation assistance, *J. Colloid Interface Sci.*, 448 (2015) 508–516.
- [41] Y. Liu, Y.J. Liu, Biosorption isotherms, kinetics and thermodynamics, *Sep. Purif. Technol.*, 61 (2008) 229–242.
- [42] K.M. Diniz, F.A. Gorla, E.S. Ribeiro, M.B.O. do Nascimento, R.J. Corrêa, C.R.T. Tarley, M.G. Segatelli, Preparation of SiO₂/Nb₂O₅/ZnO mixed oxide by sol-gel method and its application for adsorption studies and on-line preconcentration of cobalt ions from aqueous medium, *Chem. Eng. J.*, 239 (2014) 233–241.

- [43] K.Y. Foo, B.H. Hammed, Insights into the modeling of adsorption isotherm systems, *Chem. Eng. J.*, 156 (2010) 2–10.
- [44] L. Yu, Some consideration on the Langmuir isotherm equation, *Colloids Surf., A*, 274 (2006) 34–36.
- [45] F.M. de Oliveira, B.F. Somera, E.S. Ribeiro, M.G. Segatelli, M.J.S. Yabe, E. Galunin, C.R.T. Tarley, Kinetic and isotherm studies of Ni²⁺ adsorption on poly(methacrylic acid) synthesized through a hierarchical double-imprinting method using a Ni²⁺ ion and cationic surfactant as templates, *Ind. Eng. Chem. Res.*, 52 (2013) 8550–8557.
- [46] T.D. Çiftçi, E. Henden, Nickel/nickel boride nanoparticles coated resin: a novel adsorbent for arsenic(III) and arsenic(V) removal, *Powder Technol.*, 269 (2015) 470–480.
- [47] H.T. Fan, X. Fan, J. Li, M. Guo, D. Zhang, F. Yan, T. Sun, Selective removal of arsenic(V) from aqueous solution using a surface-ion-imprinted amine-functionalized silica gel sorbent, *Ind. Eng. Chem. Res.*, 51 (2012) 5216–5223.
- [48] U. Shafique, A. Ijaz, M. Salman, W.U. Zaman, N. Jamil, R. Rehman, A. Javaid, Removal of arsenic from water using pine leaves, *J. Taiwan Inst. Chem. Eng.*, 43 (2012) 256–263.
- [49] C. Gérente, Y. Andres, G. McKay, P. Le Cloirec, Removal of arsenic(V) onto chitosan: from sorption mechanism explanation to dynamic water treatment process, *Chem. Eng. J.*, 158 (2010) 593–598.
- [50] D. Ranjan, M. Talat, S.H. Hasan, Biosorption of arsenic from aqueous solution using agricultural residue ‘rice polish’, *J. Hazard. Mater.*, 166 (2009) 1050–1059.
- [51] M.J. Jiménez-Cedillo, M.T. Olguin, C. Fall, A. Colín, Adsorption capacity of iron- or iron–manganese-modified zeolite-rich tuffs for As(III) and As(V) water pollutants, *Appl. Clay Sci.*, 54 (2011) 206–216.
- [52] A.W. Samsuri, F. Sadegh-Zadeh, B.J. Seh-Bardan, Adsorption of As(III) and As(V) by Fe coated biochars and biochars produced from empty fruit bunch and rice husk, *J. Environ. Chem. Eng.*, 1 (2013) 981–988.
- [53] S.S. Tripathy, A.M. Raichur, Enhanced adsorption capacity of activated alumina by impregnation with alum for removal of As(V) from water, *Chem. Eng. J.*, 138 (2008) 179–186.